MMA Memo 209: 183 GHz radiometric phase correction for the Millimeter Array

O. P. Lay
Radio Astronomy Laboratory, University of California, Berkeley
olay@astro.berkeley.edu

May 14, 1998

Abstract

Radiometry can be used to correct the wavefront distortions of millimeter and submillimeter signals introduced by the irregular distribution of water vapor in the Earth's troposphere. By measuring the emission due to water vapor along a line of sight it is possible to estimate the corresponding electrical path length. A correction system based on the strong water vapor transition at 183 GHz is considered.

Simulations of the line profile show that this transition is at least partially saturated under even the driest conditions expected at the Chajnantor site in Chile. Potential errors in the radiometric correction process, including gain fluctuations, uncertainty in the altitude of the water vapor fluctuations, clouds, temperature fluctuations and spillover are analyzed. It is shown that the line saturation is actually beneficial, as it allows the spectral signature of a water vapor fluctuation to be discriminated from the various error components. Three or more channels are needed for this, but only moderate gain stability ($\sim 1\%$) is required, greatly easing the level of calibration necessary. Correcting the path to 50 μm is much easier to achieve when the column of water vapor is low (1 mm of Precipitable Water Vapor) than when it is high (PWV > 4 mm); the latter case requires a cooled radiometer to achieve the necessary sensitivity.

Various practical implementations are also considered, including the relative benefits of cooled and uncooled systems, and the use of dedicated radiometers versus the astronomical receivers for measuring the water line.

1 Introduction

1.1 Atmospheric Water Vapor

Fluctuations in the electrical path length through the atmosphere limit the spatial resolution and sensitivity that can be achieved by millimeter- and submillimeter-wave arrays. For the MMA to realize its full potential, it is vital that these fluctuations can be corrected.

The fluctuations are due predominantly to water vapor, which is poorly mixed in the atmosphere and has a high refractive index – both a result of the polar nature of the water molecule. The general distibution of water vapor falls off exponentially with altitude, with a scale height of ~ 2 km (compared to 8 km for the dry air component), although it is likely that this varies with convective activity in the troposphere. The precipitable water vapor (PWV) column at the Chajnantor site in Chile, measured with a 225 GHz tipping radiometer, varies from 0.5 mm under the very best conditions to over 4 mm. These are for zenith and must be scaled by the appropriate airmass at other elevations. A water vapor column of 8 mm is certainly possible for observations at low elevations, and will be adopted here as the extreme case.

Each 1 mm of precipitable water vapor increases the electrical path length through the atmosphere by about 6 mm, although the exact conversion depends on the temperature and pressure of the water vapor. Following Carilli, Lay & Sutton (1998), the benchmark accuracy adopted here for the path correction is 50 μm on each baseline. This gives a coherence of 95% at 300 GHz, and 85% at 600 GHz. A column of

8 mm PWV adds approximately 50 mm to the propagation path, so that 50 μm represents 0.1% of the total water vapor path in this extreme case. With the high opacity of a large water vapor column, however, it is likely that longer wavelength observations would be made under these conditions and the 50 μm goal could be relaxed somewhat.

1.2 Water Vapor Radiometry

The technique of water vapor radiometry uses the emission from water vapor present in the antenna beams to estimate the excess path that this water vapor introduces and compensate for the resulting phase fluctuations at the output of the correlator. The rotational transition at 183 GHz is a prime candidate for radiometric phase correction on the MMA (Carilli, Lay & Sutton 1998). Figure 1 shows simulations of the line profile for lines of sight containing different amounts of water vapor. Also shown is the increment to the spectral line when a small extra amount of water is present in the line of sight; the extra quantity is such that it adds 50 μm to the electrical path. The 5 curves in each plot show how this incremental response depends on the altitude at which this fluctuation is introduced, as well as the PWV. It is apparent that there is saturation at the line center for even 0.5 mm PWV, and that this gives rise to a characteristic double peaked spectrum for an incremental amount of water vapor (the response from the line center is reduced because of the saturation).

A single channel radiometer produces an electrical signal (a voltage V, for example) that is proportional to the total effective brightness temperature $T_{\rm tot} = gV$, where g is the instrumental gain factor. The total effective brightness temperature is the sum of the brightness temperature of the radiation entering the input horn $T_{\rm atm}$ and the internal noise temperature of the radiometer $T_{\rm rad}$. Extra water vapor in the beam of the radiometer adds electrical path $\Delta L_{\rm H_2O}$ and increases the brightness temperature by $\Delta T_{\rm atm}$. The temperature-to-path conversion factor $C(\nu, {\rm PWV}, h)$ is given by

$$\Delta L_{\rm H_2O} = C(\nu, {\rm PWV}, h) \Delta T_{\rm atm}, \tag{1}$$

where ν is the center frequency of the radiometer channel, and h is the height of the fluctuation above the ground. The sets of 5 curves in Fig. 1 correspond to 50 $\mu{\rm m}/C$. For a baseline in an array of antennas, we wish to measure fluctuations in the difference of the electrical path lengths to the two antennas A and B, in which case $\Delta T_{\rm atm} = T_{\rm atm,A} - T_{\rm atm,B}$. Since we actually measure $\Delta T_{\rm tot}$, it is important to minimize fluctuations in both the radiometer gains and noise temperatures, which are indistinguishable from fluctuations due to water vapor.

With multi-channel radiometers we measure $T_{\rm tot,A} - T_{\rm tot,B}$ over a number of channels with center frequencies $\{\nu_{\rm i}\}$. The estimator of path fluctuations $\Delta L_{\rm H_2O}$ is now some linear combination:

$$\Delta L_{\rm H_2O} = C_\Sigma({\rm PWV}, h) \sum_{\rm i} w_{\rm i} \Delta T_{\rm tot}(\nu_{\rm i}), \tag{2}$$

where C_Σ is the temperature-to-path conversion factor that is appropriate for the set of weights $\{w_{\rm i}\}$. The goal is to find a set of channels and weights $\{\nu_{\rm i}, w_{\rm i}\}$ that is sensitive to extra path, but insensitive to the various errors that complicate the measurement. These errors are described in the next section.

2 Sources of error

In addition to the desired signal $\Delta L_{\rm H_2O}$ from water vapor, there are contributions in the measurement of the excess path from a number of errors and uncertainties. Those considered here are: (1) Thermal noise; (2) Radiometer gain changes; (3) Passband changes; (4) Height of the fluctuations; (5) Clouds; (6) Temperature fluctuations; (7) Spillover; and (8) Uncertainties in atmospheric structure.

Figure 2 shows the spectral signature of the water vapor signal and each error (except for passband changes and atmospheric structure uncertainties) for different water vapor columns. Figure 3 compares the signal and errors for three different water vapor columns. The particular parameters adopted to calculate the amplitude of these errors are given at the end of each subsection below. They are guesses at realistic values, and are really only intended for illustration. The relative importance of the various contributions might be quite different in practice.

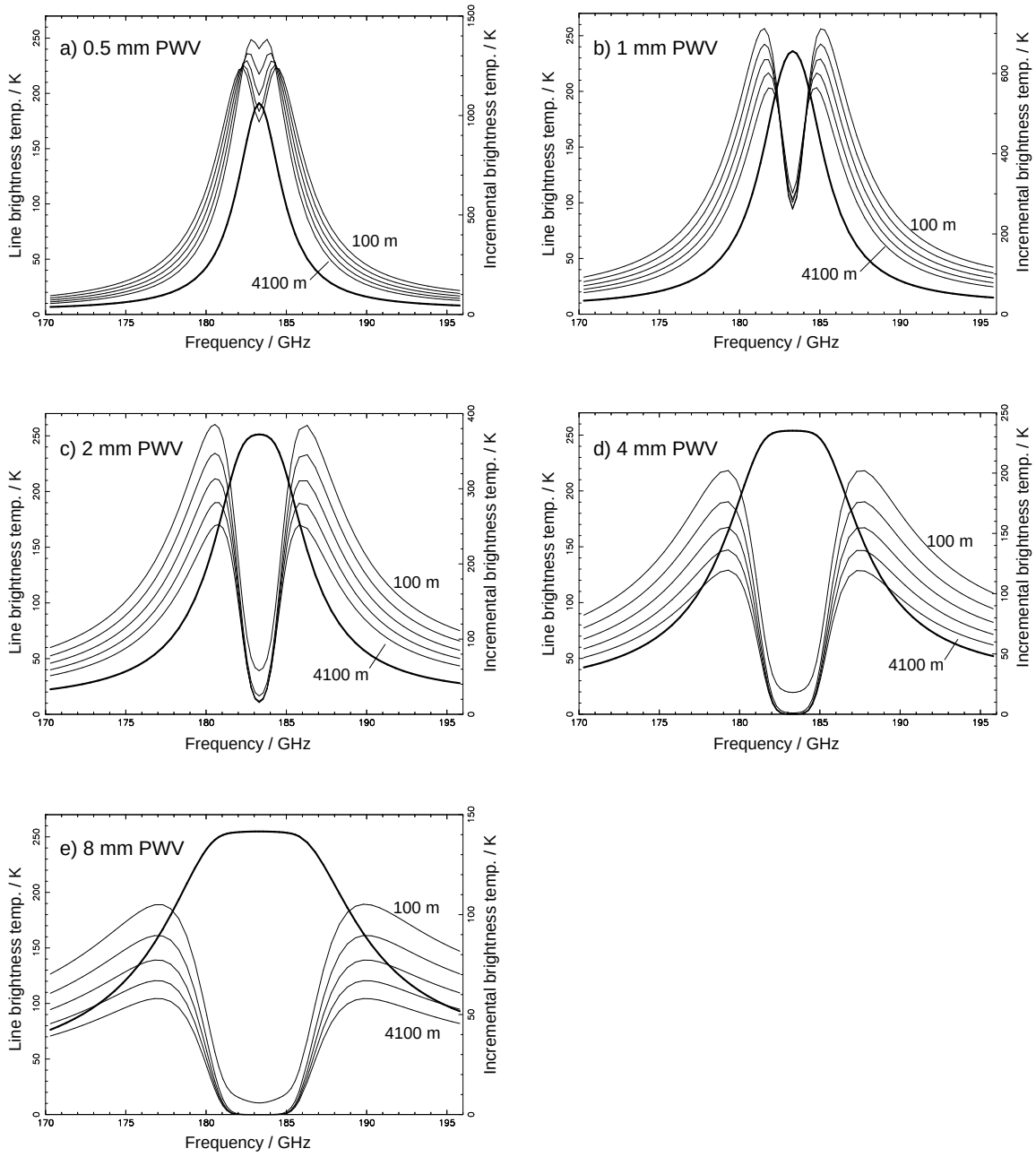

Figure 1: Thick lines: brightness temperature profiles of the 183 GHz water line for different columns of precipitable water vapor along the line of sight. Thin lines: increment in brightness temperature resulting from 50 μm of extra path at each of 5 altitudes (100 m to 4100 m above ground in steps of 1000 m). Note the change in scales for this incremental emission: case (a) has over 10 times more incremental emission than case (e). Ground level is at an altitude of 5000 m (16250 ft), the atmosphere structure is based on the U.S. Standard Atmosphere (1962) and the spectral line profiles are calculated from formulae given by Waters (1976).

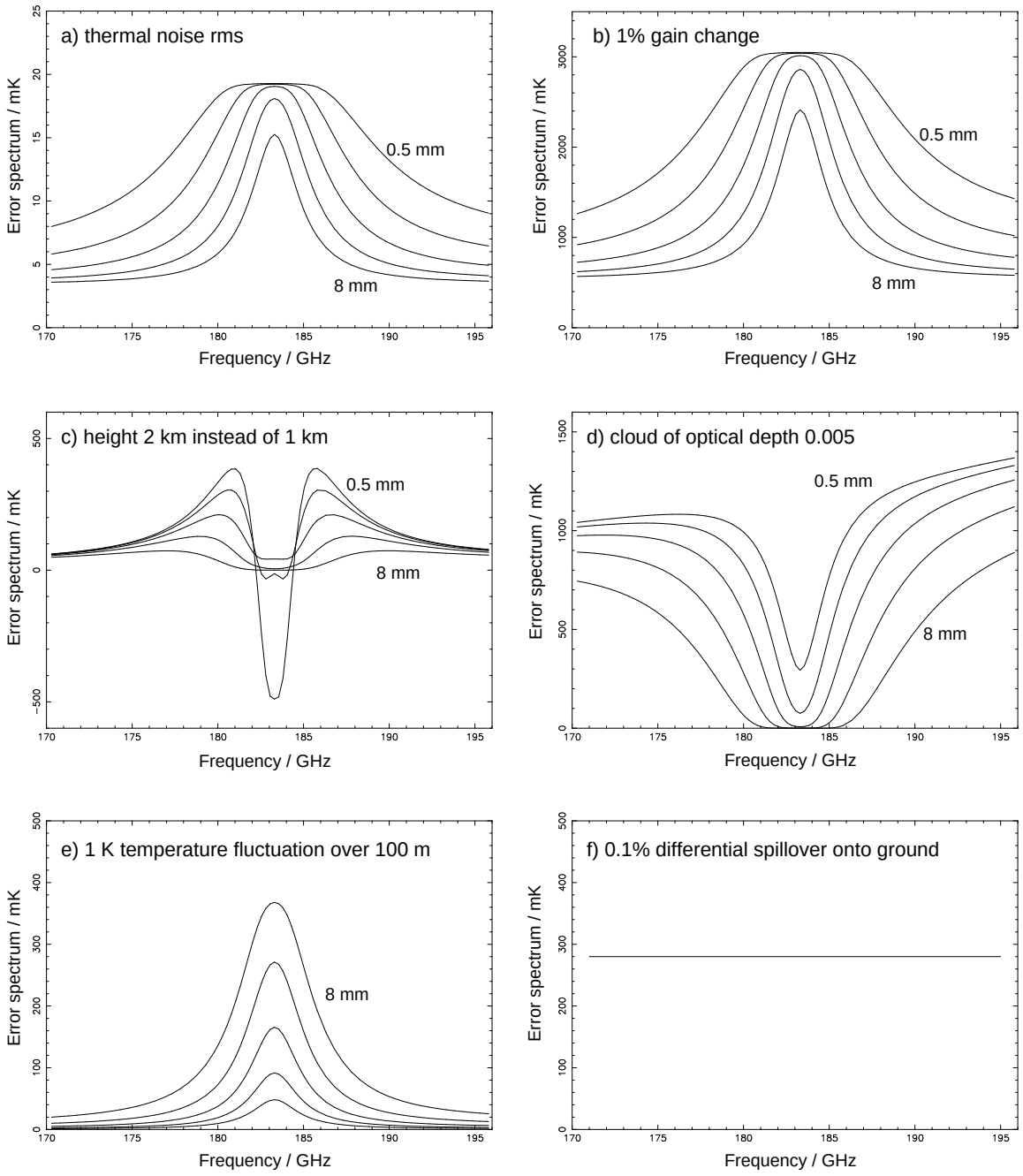

Figure 2: Spectral signature of various errors: a) thermal noise; b) radiometer gain variations; c) altitude dependence; d) clouds; e) temperature fluctuations in the atmosphere. f) spillover. The different curves in (a) to (e) show the error spectrum for 0.5, 1, 2, 4 and 8 mm of precipitable water vapor. The particular parameters used to derive these curves are listed in §2.

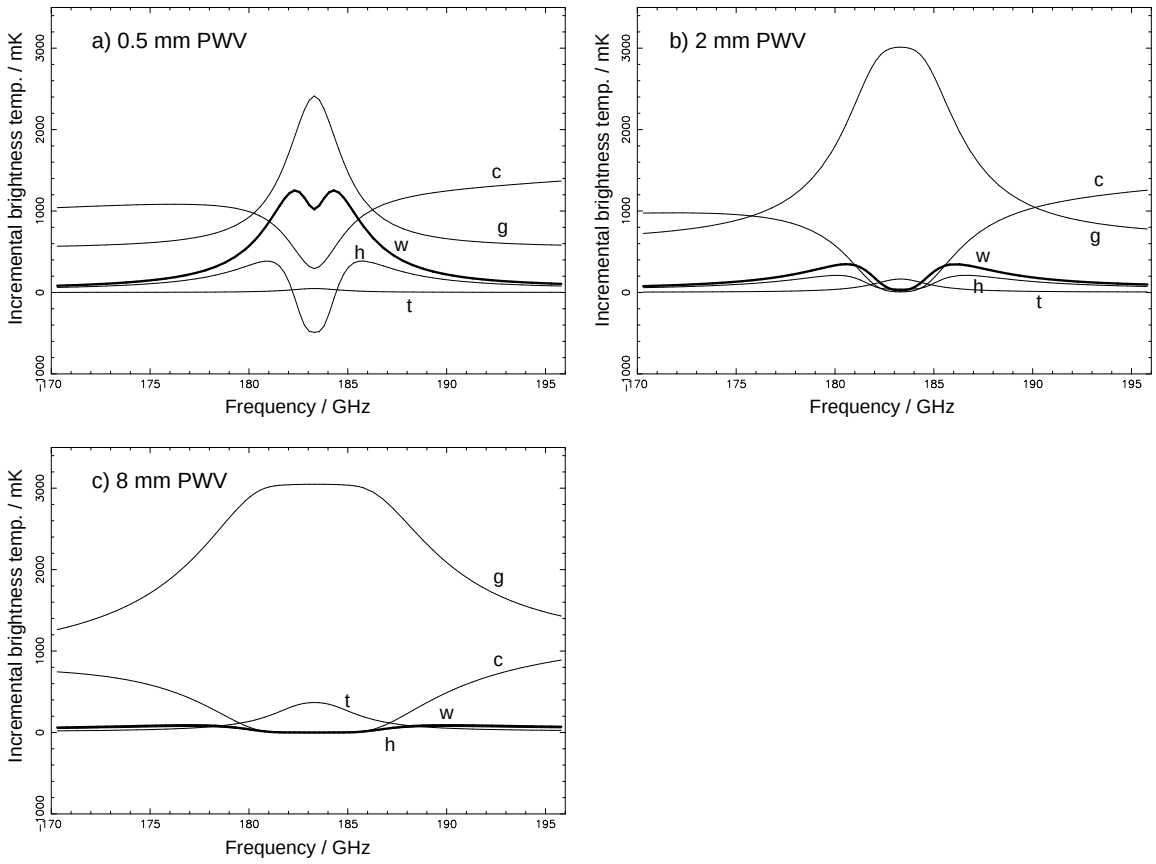

Figure 3: Comparison of different error contributions for three different water vapor columns: a) 0.5 mm PWV (excellent conditions); b) 2.0 mm PWV (average conditions); c) 8.0 mm PWV (bad conditions). Key: w = water vapor (for 50 μm extra path 1 km above the ground), g = gain change, c = cloud, h = height of fluctuations, t = temperature fluctuation. The particular parameters used to derive these curves are listed in §2.

2.1 Thermal noise

For a single channel of bandwidth $\Delta\nu$ and an integration time of t, the rms uncertainty in the excess path length due to thermal noise is given by

$$\Delta L_{\rm noise,rms} = C(\nu, {\rm PWV}, h)\,\sqrt{2}\,\frac{T_{\rm tot}(\nu)}{\sqrt{\Delta\nu t}}. \tag{3}$$

The factor of $\sqrt{2}$ accounts for the fact that the phase correction on a baseline is derived from the difference of measurements made at two antennas.

The thermal noise fluctuations are not correlated over frequency (unlike the errors discussed below), so that for a linear combination the resulting rms error is given by

$$\Delta L_{\rm noise,rms} = C_\Sigma({\rm PWV}, h)\sqrt{\sum_{\rm i}\left(\frac{2w_{\rm i}^2 T_{\rm tot}^2(\nu_{\rm i})}{\Delta\nu t}\right)}. \tag{4}$$

Figure 2a shows the rms temperature fluctuations expected for a single channel with $\Delta\nu = 500$ MHz, $t = 1$ s and $T_{\rm rad} = 50$ K (i.e. cooled radiometers). The temperature uncertainty is plotted in preference to the path uncertainty, so that the curves are also relevant to the multi-channel case where the conversion factor C_Σ depends on the channels and weights chosen.

2.2 Gain changes in the radiometers

The gain g of a radiometer or astronomical receiver is subject to fluctuations δg arising from instrument instabilities. For a one channel system, the error in the estimated path due to a gain fluctuation at one antenna is given by

$$\Delta L_{\rm gain} = C(\nu, {\rm PWV}, h)\,\frac{\Delta g}{g}\,T_{\rm tot}(\nu). \tag{5}$$

This accounts for changes in the gain that are common to all channels, e.g. those originating in the front-end mixer or IF amplifiers. Changes in the relative gains of the different channels (i.e. the passband shape) are discussed separately below. The calibration of a radiometer is simplified if as much of the gain as possible is common to all channels.

For a multi-channel system,

$$\delta L_{\rm gain} = C_\Sigma({\rm PWV}, h)\,\frac{\Delta g}{g}\,\sum_{\rm i} w_{\rm i} T_{\rm tot}(\nu_{\rm i}). \tag{6}$$

Figure 2b shows the spectral signature of a 1% gain fluctuation, assuming $T_{\rm rad} = 50$ K. In contrast to the thermal noise, the fluctuation will be common to all channels; a 1% increase in the gain will increase the measured brightness temperature in all channels by 1%.

2.3 Passband

A change in the relative gains of the channels can introduce significant errors. Since arbitrary changes can be introduced to the measured spectrum, no attempt has been made to simulate the effect. A change of 0.1% in a channel with a system temperature of 200 K would introduce a 200 mK of apparent extra brightness. Having channels as close together as possible is likely to be preferable, but this has not been taken into account in the analysis of §3.1. Calibration of the passband requires measuring the response to two loads with different temperatures.

2.4 Height of the fluctuations

It is clear from Fig. 1 that the temperature-to-path conversion factor C is a function of altitude. Consider a path length fluctuation ΔL. If the fluctuation is close to the ground, there is generally more emission than if it is at higher altitude (this is because the hotter water vapor molecules closer to the ground have a higher

random component to their rotation than the cooler molecules higher in the troposphere, resulting in a lower refractivity). For more than 1 mm of precipitable water vapor, $C(\nu, \mathrm{PWV}, 4\ \mathrm{km}) \simeq 2C(\nu, \mathrm{PWV}, 100\mathrm{m})$, for example.

The difference in measured brightness temperature for the same path length fluctuation at altitudes h_1 and h_2 is given by

$$\Delta T(\nu, \mathrm{PWV}, h_1, h_2) = \Delta L \left(C(\nu, \mathrm{PWV}, h_1)^{-1} - C(\nu, \mathrm{PWV}, h_2)^{-1} \right). \tag{7}$$

This is shown in Fig. 2c for $h_1 = 1$ km, $h_2 = 2$ km and $\Delta L = 300$ μm. The latter value is a typical rms path fluctuation level measured by the 12 GHz atmospheric phase monitor at the Chile site. The problem can be turned around to give the uncertainty in the path length estimate:

$$\Delta L_{\mathrm{alt}} = \Delta L \left(\frac{C(\nu, \mathrm{PWV}, h_2) - C(\nu, \mathrm{PWV}, h_1)}{C(\nu, \mathrm{PWV}, h_1)} \right); \tag{8}$$

i.e. if the real fluctuation ΔL is at altitude h_1, but we assume that it is at h_2, then our estimate of the fluctuation based on the change in brightness temperature will be in error by δL_{alt}.

For the single channel case, it is desirable to operate at a frequency ν where C is independent of altitude. These are called 'hinge points'. There are examples in Fig. 1a at 182.2 GHz and 184.3 GHz, which correspond to the zero crossing points in Fig. 2c for PWV = 0.5 mm. These hinge points are not present for higher water vapor columns, however.

For a multi-channel radiometer,

$$\Delta L_{\mathrm{alt}} = \Delta L \left(\frac{C_\Sigma(\mathrm{PWV}, h_2) - C_\Sigma(\mathrm{PWV}, h_1)}{C_\Sigma(\mathrm{PWV}, h_1)} \right), \tag{9}$$

and we can synthesize a hinge point by choosing a set of channels and weights $\{\nu_\mathrm{i}, w_\mathrm{i}\}$ that give a C_Σ which is independent of h. This is equivalent to finding a set of $\{\nu_\mathrm{i}, w_\mathrm{i}\}$ that give zero response to the error spectra of Fig. 2c.

2.5 Clouds

Liquid water, in the form of cloud droplets, generates a brightness temperature spectrum that basically scales as ν^2, but does not introduce significant excess path delay (Sutton and Hueckstaedt 1997). Clouds are visible above the Chajnantor site at least part of the time, and even when there appear to be no clouds, it is possible that there are diffuse clumps of small droplets present. Figure 2d shows the increment to the spectral brightness temperature profile due to a cloud that has an opacity of 0.005 at 183 GHz. The basic ν^2 contribution is modified by the higher opacity near 183 GHz due to the water vapor component.

2.6 Temperature fluctuations

Variations in temperature act on both the 'wet' and 'dry' atmospheric components. If there is a patch of atmosphere that has higher temperature than the surrounding air, then there will be extra emission from the water vapor without a significant increase in the wet refractivity. The spectra in Fig. 2e show the extra emission component from a 100 m column of air that is 1 K warmer than average.

The refractivity of dry air is also a function of temperature, and it is temperature fluctuations that limit the seeing at optical frequencies (where the refractivity of water vapor is only 5% of its value at radio wavelengths). A 1 m column of air with density 1 kg m^{-3} has an electrical path length about 200 μm longer than 1 m of vacuum. Raising the temperature decreases the density and reduces the extra path. If the atmosphere is in hydrostatic equilibrium, the total excess path is only a function of the surface pressure (Thompson, Moran and Swenson 1987), but under turbulent conditions this is no longer the case. An rms path length fluctuation of 12 μm was measured on a 13 m baseline of the Infrared Spatial Interferometer on the summit of Mount Wilson, operating at a wavelength of 11 μm (Treuhaft et al. 1995). Fluctuations of 44 μm were reported for the position of the white light fringe from a 40 m baseline of the IOTA optical interferometer on Mount Hopkins (Coudé du Foresto et al. 1998). It is not known how these measurements

should be extrapolated to the size scales relevant to the MMA, but at least some of the fluctuations must be due to water vapor.

Although the rms level of dry fluctuations is likely to be much less than that due to water vapor, it may come to dominate once the wet component has been corrected. Radiometric correction of dry fluctuations is not currently possible, and if the rms is substantially larger than 50 μm, then fast switching must be used for phase correction.

2.7 Spillover

Spillover past the edge of the primary and spillover past the edge of the secondary must both occur to some extent. In the first case, parts of the beam will be terminated on the ground and/or the sky, depending on the geometry. Spillover past the secondary is likely to be terminated on the sky, but at a different elevation from the main beam.

Spillover onto the ground produces a flat error spectrum, as shown in Fig. 2f. Since we are considering pairs of antennas, it is only the difference in the coupling of the spillover patterns to the ground that is important. For example, if antenna 1 has 0.5% of its beam terminated on the ground at 280 K, compared to 0.4% for antenna 2, the error in the differential brightness temperature is 280 mK. This error contribution will only vary slowly with time as the elevation is changed, and should be mostly removed by regular phase calibration on a nearby source.

Spillover onto the sky at a lower elevation introduces an extra component of water vapor which will change when slewing from the target source to the calibrator. For example, consider the case where antenna 1 has 0.1% of extra spillover past the top edge of the primary compared to antenna 2, which is terminated on an 8 mm column of water vapor at 10° elevation. Moving 1° in elevation from target to calibrator changes this spillover water column by about 10%, which would change the measured brightness temperature profile by about 5 mK. This is not large enough to be significant.

2.8 Atmospheric model

Measuring a total excess path of 50 mm (from 8 mm of PWV) to an accuracy of 50 μm requires a very accurate model of the temperature, pressure and water vapor distribution as a function of altitude, since the refractive index of the water vapor depends on temperature and pressure (Carilli et al. 1998). Such an accurate model is not required for phase correction on the MMA, however, since the broad distribution of water vapor (i.e. excluding the fluctuations) is common to all antennas and cancels out when differences between the antenna beams are calculated. The vertical distribution of this common component does influence the temperature-to-path conversion factor C, and is discussed in the next section.

3 Choosing channels

With only one frequency channel there is no way to distinguish between fluctuations due to water vapor and the various sources of error discussed above. Even with multiple channels, separating the signal from the errors can be difficult. This is true for radiometers that measure emission from the 22 GHz water line, where the spectral signature of extra water vapor is very similar to the spectral signature from a gain change. This is because the line is optically thin and the line amplitude is proportional to the water vapor column. The design of a 22 GHz radiometer is therefore driven by the need to minimize or calibrate out gain fluctuations, requiring tight thermal regulation of components and frequent calibration with standard loads. Even a cooled radiometer requires a gain stability of better than 0.1%, corresponding to 50 μm out of 50 mm; room temperature 22 GHz instruments need to be better than 0.01%.

The saturation of the 183 GHz line is actually a big advantage in this situation, since the spectral signature of extra water vapor is easily distinguished from the various error contributions (Fig. 3). This concept is explored quantitatively in the next section with a simple 3 channel system.

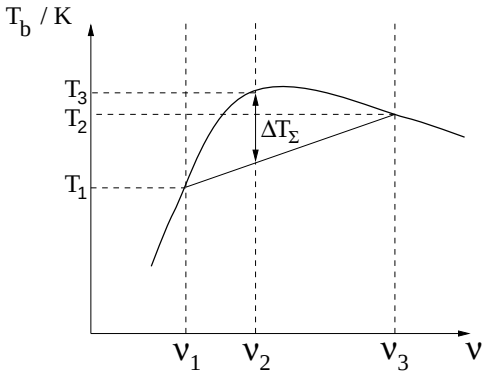

Figure 4: The response of the 3-channel linear combination described in §3.1 to an arbitrary spectral profile. The linear combination is sensitive to the deviation from a straight line.

3.1 A simple example: 3 channels

Consider a radiometer that has 3 channels at frequencies that can be adjusted to suit the prevailing conditions. There are 6 free parameters: the center frequencies of the channels ν_1, ν_2, ν_3 and the corresponding weights w_1, w_2, w_3. In order to restrict the parameter space, the weights are chosen so that the linear combination has a zero response to any brightness temperature spectrum of the form $T = A + B\nu$. Choosing

$$w_1 = -\frac{(\nu_3 - \nu_2)}{(\nu_3 - \nu_1)} \tag{10}$$

$$w_2 = +1 \tag{11}$$

$$w_3 = -\frac{(\nu_2 - \nu_1)}{(\nu_3 - \nu_1)} \tag{12}$$

has the desired result. Figure 4 illustrates graphically the response of the linear combination $\Delta T_\Sigma = w_1 T_1 + w_2 T_2 + w_3 T_3$ to an arbitrary spectral profile. The response is proportional to the net curvature between ν_1 and ν_3. A computer fitting routine takes a set of 32 channels spaced by 0.25 GHz in the range 183.3 GHz (the line center) to 191.3 GHz, and finds the combination of 3 channels that minimizes the total residual error. This is repeated for different columns of water vapor and the results are tabulated in Table 1. Figure 5 shows how this approach effectively discriminates between the signal and error terms. From Table 1 it can be seen that the optimum frequencies shift further away from the line center as the column of water vapor increases. For each water vapor column there are several channel combinations that give very similar residual errors, but only the best one has been shown. There is no fixed set of 3 channels that satisfies the 50 μm criterion under all conditions, even if the PWV = 8 mm case is ignored. In practice, the optimum combination of frequencies will also depend on the relative importance of the different error terms.

The numbers in Table 1 clearly demonstrate that estimating the excess path accurately becomes more difficult as the water vapor column increases, primarily because of the reduced signal (Fig. 1). For 0.5 mm PWV, the predicted path correction error of 6 μm is well below the benchmark goal of 50 μm; at 8 mm PWV the error has risen to 89 μm. The uncertainty resulting from changes in the passband, and from possible dry fluctuations has not been included.

The vertical structure of the atmosphere is likely to deviate from the US Standard Atmosphere used in these calculations. To investigate this, the optimum channels listed in Table 1 were used with different atmospheric models to calculate new values for the conversion factor C_Σ. It was found that neither the surface pressure nor the temperature profile have much impact, but that the scale height of the water vapor distribution is more important. The effect was most marked for PWV = 0.5 mm, where C_Σ decreased by 16% if the scale height was increased from 2.0 to 2.5 km. This problem is related to the uncertainty in the altitude of the fluctuations (§2.4) and emphasizes the need for empirical determinations of C_Σ from measurements of the phase fluctuations of bright astronomical sources.

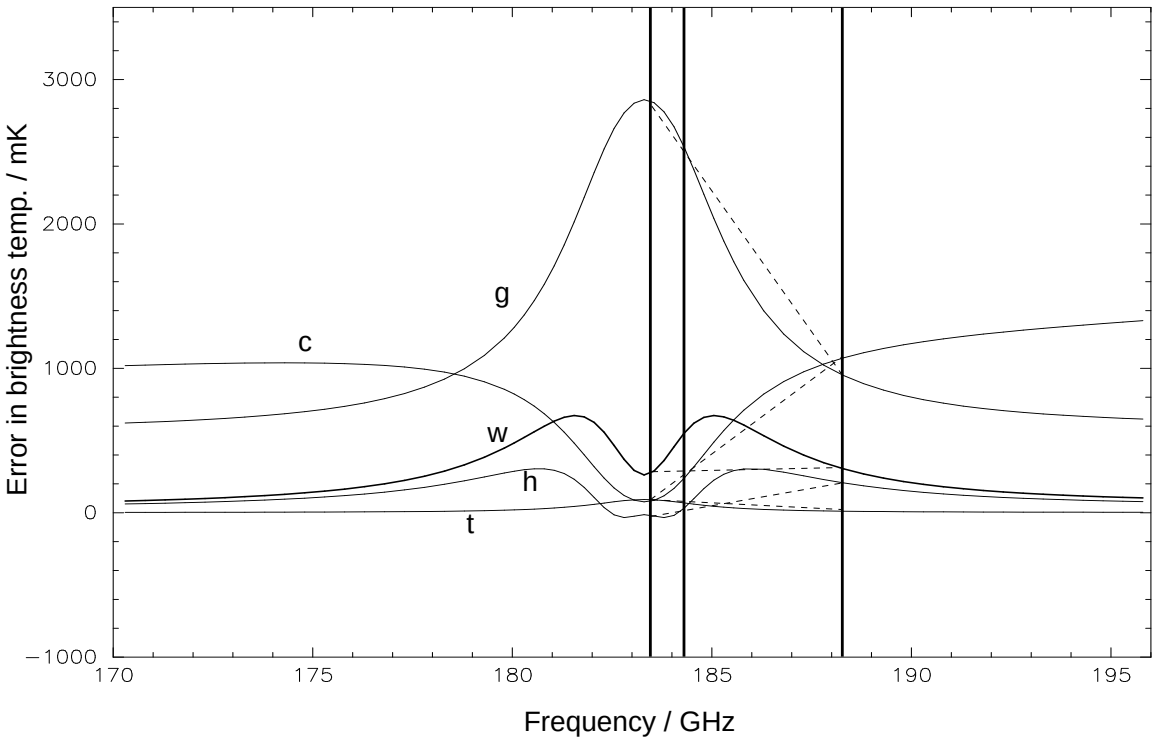

Figure 5: The response of a linear combination of 3 channels to extra water vapor and to the various error contributions (1 mm PWV). Since the weights of the channels are chosen to have a null response to a straight line, the 3 frequencies can be chosen to reject the main error terms while giving a significant response to the signal. Key: w = water vapor (for 50 μm extra path 1 km above the ground), g = gain change, c = cloud, h = height of fluctuations, t = temperature fluctuation. The particular parameters used to derive these curves are listed in §2.

Water vapor column	0.5 mm	1.0 mm	2.0 mm	4.0 mm	8.0 mm
$\{\Delta\nu_1, \Delta\nu_2, \Delta\nu_3\}$/ GHz	$\{0.0, 0.5, 5.0\}$	$\{0.25, 1.0, 5.0\}$	$\{0.5, 1.75, 7.5\}$	$\{1.75, 3.5, 5.5\}$	$\{3.0, 5.0, 7.5\}$
ΔT_Σ for 50 μm path	205 mK	256 mK	189 mK	59 mK	23 mK
Thermal noise	4 μm	4 μm	6 μm	16 μm	43 μm
Gain change	3 μm	1 μm	1 μm	5 μm	21 μm
Altitude uncert.	2 μm	3 μm	17 μm	35 μm	44 μm
Cloud emission	2 μm	1 μm	4 μm	5 μm	8 μm
Temperature	1 μm	2 μm	11 μm	25 μm	61 μm
Ground spillover	0	0	0	0	0
Total uncert.	6 μm	6 μm	21 μm	46 μm	89 μm

Table 1: Optimum combination of 3 channels for each water vapor column. The total uncertainty in the excess path consists of independent contributions from the listed specific error terms (see §2 for details). Passband variations and dry fluctuations have not been included.

The 3 channel example discussed above was chosen to illustrate how the signal spectral signature may be discriminated from the various error terms. The main conclusions are:

- The saturation of the 183 GHz line is a beneficial, allowing the water vapor signal to be distinguished spectrally from the possible errors.
- At least 3 frequency channels are required to separate the signal from the error terms.
- The frequencies need to be varied to suit the conditions.
- For low columns of water vapor (PWV < 4 mm) the residual path error is less than 50 μm.
- For higher water vapor columns the high saturation leads to a small signal and the error contributions become large.

3.2 General Case

A radiometer with many channels will, in general, be superior to one with few channels, since there is more information available for making the correction. Consider an instrument with many channels, equally spaced over the line. The path correction is estimated by

$$\Delta L = C_\Sigma \sum_{\rm i} w_i \Delta T(\nu_{\rm i}), \tag{13}$$

where $\Delta T(\nu_{\rm i})$ is the difference in brightness temperature measured by two radiometers in the channel centered on $\nu_{\rm i}$. In practice, an algorithm is required that takes all of the available information (e.g. the measured water line profile; temperature, pressure and humidity at ground level; best estimates of the importance of the various error terms) and calculates the optimum set of weights w_i appropriate for the conditions. The most important term will be the column of water vapor along the line of sight which can be determined from the line profile; the other factors provide refinements. Although theoretical lineshapes provide a starting point for such an algorithm, it is likely that empirical measurements of the phase fluctuations measured for strong astronomical sources will provide continuous adaptation and improvement.

4 Practical implementation

Several options are considered for the 183 GHz radiometer front-end:

1. Standalone uncooled radiometer.
2. Standalone cooled radiometer
3. Dedicated radiometer in main dewar
4. Astronomical receiver as a radiometer

The pros and cons of each possibility are examined in the next section. Back-end spectrometers are discussed briefly in §4.5.

4.1 Standalone uncooled radiometer

+ Does not take up valuable dewar space.
– High thermal noise contribution (see below).
– Demanding calibration requirements (see below).
– Pick-off mirror needed to couple the radiometer to the sky via the secondary and primary mirrors. Must not interfere with any of the astronomical beams.

A typical receiver temperature for a room temperature Schottky system is of order 2000 K, giving an rms thermal noise of 90 mK for a 1 s integration and 0.5 GHz of bandwidth. This is not sufficient to measure the values of ΔT given in Table 1 for 4 mm or 8 mm of water vapor. An integration time of 10 s would reduce the noise by a factor of 3, but it is likely that some fraction of the time would have to be spent on calibration against reference loads. With a system temperature of 2000 K, small changes in the passband (the gain of one channel relative to the others) can introduce significant errors. The relative gains of the channels need to be known to within approximately 0.002%. This is a very demanding level of calibration, requiring two loads, one of which must be cold (in order to achieve a significant temperature differential).

4.2 Standalone cooled radiometer

+ Does not take up valuable dewar space.
+ Has sufficient sensitivity when the water vapor column is large.
+ Calibration requirements are more tractable than uncooled system (although passband stability of 0.01% is required for 8 mm of water vapor).
− Extra expense, space and complication of another dewar in the antenna cabin.
− Pick-off mirror needed.

4.3 Dedicated radiometer in main dewar

− Takes up valuable dewar space.
− Extra expense and maintenance.
+ Has sufficient sensitivity when the water vapor column is large.
+ Calibration requirements are more tractable than uncooled system (although passband stability of 0.01% is required for 8 mm of water vapor).
− Difficult to have a warm load calibration that is independent of the astronomy system. A warm load could be shared, but the calibration interval would be driven by the radiometry requirement, rather than the astronomy.

4.4 Astronomical receiver as a radiometer

+ No extra expense on front-ends.
+ No extra dewar space used for radiometry.
+ Has sufficient sensitivity when the water vapor column is large.
+ Calibration requirements are more tractable than uncooled system (although passband stability of 0.01% is required for 8 mm of water vapor).
+ A sideband separating receiver might make passband calibration much easier.
− Difficult to have a warm load calibration that is independent of the astronomy system. A warm load could be shared, but the calibration interval would be driven by the radiometry requirement, rather than the astronomy.

There are at least two possible ways in which the receivers might be used:

a) Parallel Operation. One receiver is used for the astronomical observations and one is used for monitoring the 183 GHz water line. Two receivers are needed that are capable of measuring 183 GHz so that simultaneous astronomy and radiometry are possible at all frequencies (i.e. the bands of 140 GHz and 230 GHz receivers should overlap).

- Requires two LO systems for dual operation.
- \+ Continuous coverage of the atmospheric fluctuations.

b) Time-multiplexed operation. Only one receiver is used at a given time. Receivers are switched whenever a radiometric measurement is needed. For example, the astronomy receiver would be used for 9 s, then receivers are switched for 1 s to do radiometry, then back to the astronomical receiver. The cycling time would be set to suit the conditions, but in general most of the fluctuation power is on the longer timescales. Assuming the radiometric correction is accurate, this approach would give superior results compared to fast switching between target source and calibrator with the same cycle time (where there is generally a spatial offset on the sky, the integration time on the calibrator must be long enough to obtain a good phase measurement, and there is time lost to slewing).

- Does not correct for very fast fluctuations (although this should be only a small contribution).
- A fraction of the potential astronomical observing time is lost.
- \+ Requires no extra LO system.
- \+ IF signals can be sent to a central location using the existing IF optical fiber.
- Requires that receivers and LO can be switched rapidly.

4.5 Back-end options

A spectrometer covering approximately 8 GHz of IF bandwidth with a resolution of order 0.5 GHz is needed for each radiometer. The passband should be very stable. Either a filterbank or an analog lag autocorrelator (e.g. Harris, Isaak and Zmuidzinas 1998) could provide ∼16 equally spaced channels across the band. Alternatively, a fewer number of tunable channels could be used. In the extreme case one channel could be switched rapidly between several different frequencies. This would be at the expense of the signal-to-noise ratio, but with a potentially very stable passband.

5 Summary

1. Simulations of the 183 GHz water line show that the line is at least partially saturated under even the driest conditions (PWV = 0.5 mm) expected at the Chajnantor site.

2. This saturation results in a characteristic double-peaked spectral signature from a water vapor fluctuation.

3. The spectral signatures resulting from gain fluctuations, uncertainties in the altitude of the fluctuations, clouds, temperature fluctuations and spillover are also simulated.

4. With three channels, it is possible to discriminate effectively between the double-peaked signal and the various error contributions. In particular, the impact of gain fluctuations can be substantially reduced, and gain changes of at least 1% are allowable. This greatly simplifies the radiometer calibration requirements. The relative gains of the channels with respect to one another must be stable to within 0.01% (for a PWV column of 8 mm), however. The optimum frequencies of the channels are a function of the column of water vapor.

5. With a set of ∼16 fixed 500 MHz channels going out to 8 GHz from the line center, it should be possible to make a very good correction for water vapor. It is possible, however, that temperature fluctuations acting on the dry air component (responsible for poor seeing at optical wavelengths) will determine the residual error. Little is currently known about the structure function of these dry fluctuations on large scales.

6. Estimating the excess path to an accuracy of 50 μm requires cooled radiometers when the water vapor column is 4 mm or more.

7. The pros and cons of using the astronomical receivers instead of dedicated radiometers was also discussed.

References

Carilli, C. L., Lay, O. P., & Sutton, E. C. 1998, "Radiometric Phase Correction", MMA White Paper

Coudé du Foresto, V., Perrin, G., Mariotti, J., Lacasse, M. G., & Traub, W. A. 1998, "FLUOR/IOTA Stellar Interferometer", Proc. of SPIE Vol. 3350, eds. R. D. Reasenberg & J. B. Breckenridge

Harris, A. I., Isaak, K. G., & Zmuidzinas, J. 1998, "WASP: wideband analog correlator spectrometer", Proc. of SPIE Vol. 3357, ed. T. G. Phillips

Sutton, E. C., & Hueckstaedt, R. M. 1997, "Radiometric monitoring of atmospheric water vapor as it pertains to phase correction in millimeter interferometry", A&A Supp., 119, 559

Thompson, A. R., Moran, J. M., & Swenson, G. 1986, Interferometry and Synthesis is Radio Astronomy, New York: Wiley

Treuhaft, R. N., Lowe, S. T., Bester, M., Danchi, W. C., & Townes, C. H. 1995, "Vertical Scales of Turbulence at the Mount Wilson Observatory", ApJ, 453, 522